Why CO_2 cools the middle atmosphere – a consolidating model perspective

Helge F. Goessling[1] and Sebastian Bathiany[2]

[1]Alfred Wegener Institute, Helmholtz Centre for Polar and Marine Research, Bremerhaven, Germany
[2]Wageningen University, Wageningen, Netherlands

Correspondence to: Helge F. Goessling (helge.goessling@awi.de)

Abstract. Complex models of the atmosphere show that increased carbon dioxide (CO_2) concentrations, while warming the surface and troposphere, lead to lower temperatures in the stratosphere and mesosphere. This cooling, which is often referred to as "stratospheric cooling", is evident also in observations and considered to be one of the fingerprints of anthropogenic global warming. Although the responsible mechanisms have been identified, they have mostly been discussed heuristically, incompletely, or in combination with other effects such as ozone depletion, leaving the subject prone to misconceptions. Here we use a one-dimensional window-grey radiation model of the atmosphere to illustrate the physical essence of the mechanisms by which CO_2 cools the stratosphere and mesosphere: (i) the *blocking effect*, associated with a cooling due to the fact that CO_2 absorbs radiation at wavelengths where the atmosphere is already relatively opaque, and (ii) the *indirect solar effect*, associated with a cooling in places where an additional (solar) heating term is present (which on Earth is particularly the case in the upper parts of the ozone layer). By contrast, in the grey model without solar heating within the atmosphere, the cooling aloft is only a transient blocking phenomenon that is completely compensated as the surface attains its warmer equilibrium. Moreover, we quantify the relative contribution of these effects by simulating the response to an abrupt increase in CO_2 (and chlorofluorocarbon) concentrations with an atmospheric general circulation model. We find that the two permanent effects contribute roughly equally to the CO_2-induced cooling, with the indirect solar effect dominating around the stratopause and the blocking effect dominating otherwise.

1 Introduction

The laws of radiative transfer in the Earth's atmosphere are a key to understand our changing climate. With the absorption spectra of greenhouse gases as one central starting point, climate models of increasing complexity have been built during the last decades. These models show that increased carbon dioxide (CO_2) concentrations, while warming the surface and the troposphere, lead to lower temperatures in the middle atmosphere (MA; the stratosphere and the mesosphere) (Manabe and Strickler, 1964; Manabe and Wetherald, 1967, 1975; Fels et al., 1980; Gillett et al., 2003). Meanwhile, observations show a cooling trend in the MA during the satellite era until the most recent years; the negative trend is especially large in the upper stratosphere and in the mesosphere, although uncertainties also increase with height (Beig et al., 2003; Randel et al., 2009; Liu and Weng, 2009; Beig, 2011; Seidel et al., 2011; Thompson et al., 2012; Huang et al., 2014).

Attribution studies have concluded that the depletion of stratospheric ozone was probably the main driver of the cooling in the lower stratosphere (Ramaswamy and Schwarzkopf, 2002; Shine et al., 2003; Thompson and Solomon, 2005, 2009; Forster et al., 2007; Santer et al., 2012), especially in the Antarctic spring (Ramaswamy et al., 2001; Thompson and Solomon, 2009). In addition, the roles of volcanoes and atmospheric dynamics (Thompson and Solomon, 2009), stratospheric water vapour (Ramaswamy et al., 2001; Shine et al., 2003; Maycock et al., 2011; Seidel et al., 2011), and climate variability (Seidel et al., 2011) have been discussed. The increase of CO_2 concentration contributed to the decrease of lower stratospheric temperatures, but only to a small extent (Shine et al., 2003). In the middle and upper stratosphere (and beyond), the CO_2 increase has probably been the most important reason for the temperature decrease (Ramaswamy et al., 2001; Ramaswamy and Schwarzkopf, 2002; Shine et al., 2003; Thompson and Solomon, 2005). As ozone concentrations are expected to recover in the future, it seems likely that CO_2-concentrations will be of growing importance also in the lower stratosphere (Stolarski et al., 2010; Ferraro et al., 2015).

The isolated effect of CO_2 on temperatures in the MA is rarely explained. Probably the most frequent argument found in textbooks (e.g., Pierrehumbert, 2010; Neelin, 2011) is related to the ozone layer where a considerable part of the locally absorbed radiation is short-wave (solar) radiation. Therefore, the temperature around the stratopause exceeds the corresponding temperature in a hypothetical grey atmosphere by far. Because the main absorption bands of CO_2 are in the long-wave (LW) part and not in the solar part of the spectrum, an increase in CO_2 leads to increased emission of LW radiation while the rate of solar heating remains unaltered. The excess of emission compared to absorption leads to a cooling. It should be stressed that the argument is related not to the depletion but to the mere presence of ozone (Ramaswamy and Schwarzkopf, 2002). Although this effect is a major contributor to CO_2-induced MA cooling (as we confirm below), this explanation is less convincing in the middle and upper mesosphere where there is unabated (observed and simulated) cooling despite the solar heating becoming weaker with height. Neither can this effect explain an important difference between CO_2 and other long-lived greenhouse gases: While methane and nitrous oxide have a much weaker effect on MA temperatures compared to CO_2, chlorofluorocarbons (CFCs) even tend to warm the lower stratosphere (neglecting ozone depletion) (Dickinson et al., 1978; Forster and Joshi, 2005).

More complete explanations discern not only between solar and LW radiation, but treat the LW absorption spectra of greenhouse gases in more detail. Ramaswamy et al. (2001) and Seidel et al. (2011) point out that the balance of LW emission and LW absorption must be considered: Any greenhouse gas emits simply according to its local temperature, but absorbs radiation emitted from certain distances (represented by radiation mean free paths) depending on the absorption spectrum of the gas and the atmospheric composition. At the absorption bands of certain CFCs, the radiation mean free path of the atmosphere is large because the bands are located in the spectral window region. These CFCs thus absorb mainly radiation emitted from the warm surface and lower troposphere, but emit with the low temperatures of the MA. Consequently, increased CFC concentrations impose a LW warming tendency. Ramaswamy et al. (2001) point out that, in contrast, the radiation mean free path in the $15\,\mu m$ band of CO_2 is small, implying that the radiation absorbed by CO_2 in the MA mainly comes from the cold tropopause region.

Forster et al. (1997b) and Ramaswamy et al. (2001) address yet another aspect: The MA responds much faster than the rather inert surface-troposphere system. Hence, when greenhouse gases are added to the atmosphere, initially the MA cools because the radiation mean free path of the atmosphere has been reduced and the radiation arriving in the MA now stems from higher,

colder levels of the troposphere. After this first phase of MA temperature adjustment, the surface and troposphere gradually warm, leading to increased upward LW radiation at the tropopause which warms the lower stratosphere.

All these effects, though mentioned in the literature and included in complex climate models, are rarely discussed together. Furthermore, they are usually explained only heuristically and not demonstrated with a conceptual model. The most popular educational model of the greenhouse effect, a global-mean grey atmosphere model with one ground level and a one-layer atmosphere (e.g., Neelin, 2011; Liou, 2002), can not explain CO_2-induced MA cooling. Although Thomas and Stamnes (1999) introduce an atmospheric window to their conceptual model, they do not apply it to explain MA cooling. The same is true for more complex conceptual models (e.g., Pollack, 1969a, b; Sagan, 1969; Pujol and North, 2002), which are also not limited to the ingredients needed to explain how CO_2 cools the MA.

Our article aims to provide a consolidating model perspective on CO_2-induced MA cooling. The first part has an educational emphasis as we demonstrate the physical essence of the mechanisms involved, using simple variants of a vertically continuous global-mean radiation model: In Sect. 2 we derive the grey atmosphere model from the general radiative transfer equation, in close analogy to such models in the educational literature (e.g., Goody and Yung, 1989; Thomas and Stamnes, 1999). The grey atmosphere model features no permanent MA cooling when applied in its pure form. In Sect. 3 we therefore extend the grey model to the simple case of two LW bands of which one is fully transparent, i.e., the window-grey case. The rigorous derivations in Sects. 2 and 3 may be skipped by readers primarily interested in the resulting explanations. In Sect. 4 we explain CO_2-induced MA cooling using the window-grey radiation model. In Sect. 5 we provide a quantitative separation of the effects based on simulations with the atmospheric general circulation model ECHAM6. Based on these simulations we discuss what can, and what can not, be learnt about the effect strengths based on the window-grey model. This is followed by a summary and conclusions in Sect. 6. In addition to our model derivations, Appendix A offers a simple analogy to understand the blocking effect of CO_2 without any equations. Moreover, we show the relation of the vertically continuous model to discrete-layer models in Appendix B and provide a formal response analysis in terms of partial derivatives with respect to the parameters of the window-grey model in Appendix C. Appendix D provides technical details on Fig. 1.

2 The grey-atmosphere model

In the following we derive the vertical temperature profile of a grey atmosphere, first with only the atmosphere in thermal equilibrium and then assuming equilibrium also for the surface. We consider a vertically continuous grey atmosphere with horizontally homogeneous (global-mean) conditions. The grey atmosphere is transparent for solar radiation and uniformly opaque for LW radiation. Splitting the electromagnetic spectrum into a transparent solar band and an opaque LW band is a common approximation that is naturally suggested by (i) the well separated emission spectra of the Sun and the Earth (Fig. 1a) and (ii) the shape of the absorption spectrum of the Earth's atmosphere (Fig. 1b). The grey model accounts only for radiation while other processes of energy transfer (most importantly convection) are neglected. Greenhouse gases are assumed to be well-mixed and any effects from clouds or aerosols are neglected. Assuming horizontally homogeneous conditions and the absence of scattering we apply the two-stream approximation (Liou, 2002; Pierrehumbert, 2010), meaning that we distinguish only

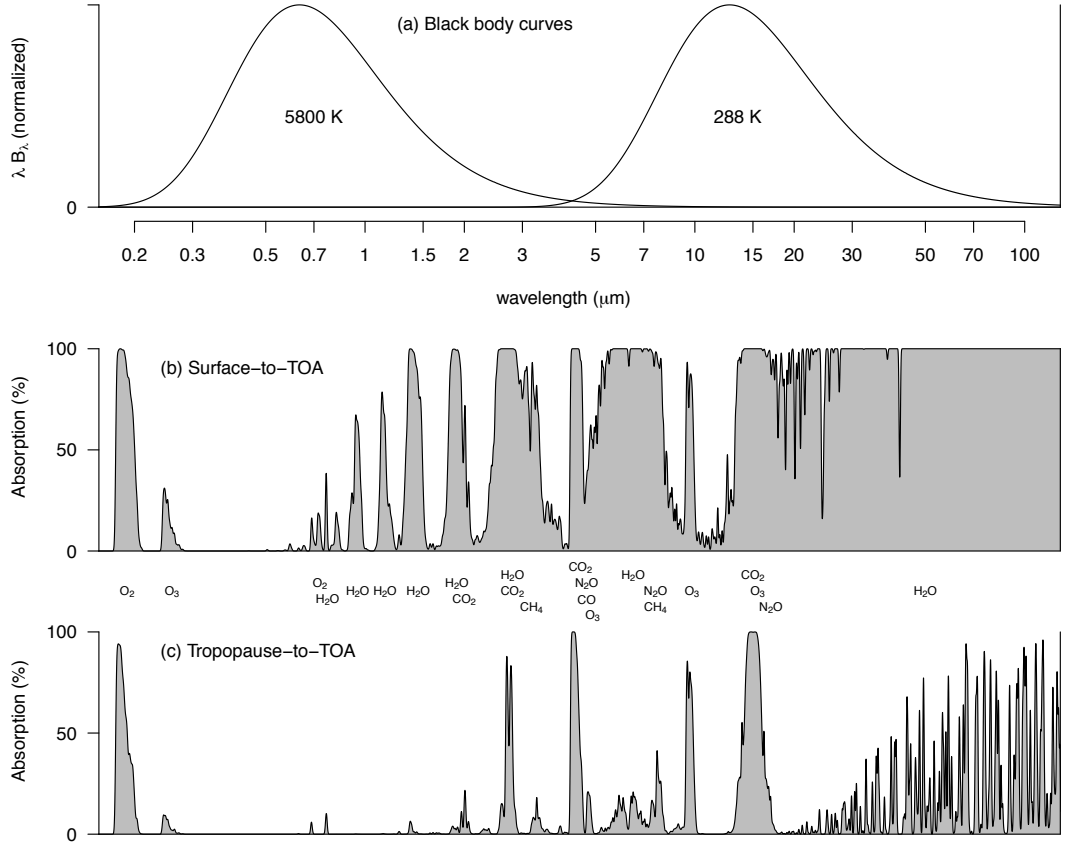

Figure 1. (a) Normalized black body curves for 5800 K (the approximate emission temperature of the Sun) and 288 K (the approximate surface temperature of the Earth). (b) Representative absorption spectrum of the Earth's atmosphere for a vertical column from the surface to space, assuming the atmosphere to be a homogeneous slab. (c) The same but for a vertical column from the tropopause ($\sim$11 km) to space. Spectra based on *HITRAN on the Web*; see Appendix D for details. Figure after Goody and Yung (1989, Fig. 1.1 on p. 4).

upward and downward propagating radiation (indicated by arrows in the subsequent equations). This leads to the differential form of the radiative transfer equation (e.g., Goody and Yung, 1989; Pierrehumbert, 2010)

$$\frac{\mathrm{d}L^{\uparrow}(z)}{\mathrm{d}z} = \frac{1}{\mu}\left[J - L^{\uparrow}(z)\right]\rho(z)\,k \tag{1}$$

with radiance L, source term J, geometric height z, air density ρ, mass absorption coefficient k, and $\mu = cos(\theta)$ with the effective angle of propagation θ. To remove any angular dependence from the equations, we use the common assumption of an effective angle of propagation of 60° relative to the vertical, i.e., $\mu = 1/2$ (see Pierrehumbert, 2010, Chapter 4.2). As we

neglect scattering, J only consists of the long-wave blackbody emission, which is isotropic. Integrating Eq. (1) over the half sphere then yields

$$\frac{\mathrm{d}F^{\uparrow}(z)}{\mathrm{d}z} = \left[\sigma\, T(z)^4 - F^{\uparrow}(z)\right] \rho(z)\, k \tag{2}$$

with irradiance F (in W/m^2) and the Stefan-Boltzmann constant σ. Using the relative pressure deficit

$$h = 1 - p/p_{srf} \tag{3}$$

as vertical coordinate, where p is pressure and p_{srf} is surface pressure, the radiative transfer equation reads

$$\frac{\mathrm{d}F^{\uparrow}(h)}{\mathrm{d}h} = \left[\sigma\, T(h)^4 - F^{\uparrow}(h)\right] \alpha\,. \tag{4}$$

The absorption coefficient α is the only parameter of the grey model and describes the atmospheric opacity in the LW band. Due to our definition of the vertical coordinate h, α is independent of h (in fact, it follows from hydrostatic balance that $\alpha = k\, p_{srf}/g$). Also, h is proportional to optical thickness: $\tau = \alpha\, h$. Although we distinguish the parameter α from the vertical coordinate h, our model is equivalent to similar approaches in popular textbooks of radiative transfer which usually choose optical depth (τ, also called optical thickness) as their vertical coordinate. For example, the optical thickness between a height h and the top of the atmosphere, in our case $\alpha(1-h)$, is identical to $\tau_\infty - \tau$ in Pierrehumbert (2010), to τ in Salby (1992), and to $\tau/\overline{\mu}$ in Thomas and Stamnes (1999). In the latter two cases, the vertical axis points downwards, hence the reversed sign. In Thomas and Stamnes (1999), a parameter $\overline{\mu}$ still appears in the equations as no assumption on the average direction of propagation is made.

Equation (4) is the spectrally integrated grey-absorption-case of Schwarzschild's equation and holds analogously for downwelling LW radiation $F^{\downarrow}$. In radiative equilibrium F must be free of divergence because other source or sink terms of heat are neglected. With $F^{\downarrow}_{toa} = 0$, $F^{\downarrow}$ is hence determined by

$$F^{\uparrow}(h) - F^{\downarrow}(h) = F^{\uparrow}_{toa}\,, \tag{5}$$

where the index *toa* stands for the top of the atmosphere (TOA). Thermal equilibrium for a thin layer of air is given when

$$2\,\epsilon\,\sigma\, T(h)^4 = \epsilon\, \left(F^{\uparrow}(h) + F^{\downarrow}(h)\right)\,, \tag{6}$$

where $\epsilon = \alpha\, \mathrm{d}h$ is the emissivity, and hence also the absorptivity, of the thin layer for LW radiation. Combining Eqs. (5) and (6) yields

$$\sigma\, T(h)^4 = F^{\uparrow}(h) - \frac{F^{\uparrow}_{toa}}{2}\,. \tag{7}$$

Substituting Eq. (7) into the radiative transfer equation (Eq. (4)) gives

$$\frac{\mathrm{d}F^{\uparrow}(h)}{\mathrm{d}h} = -\frac{\alpha}{2}\,F^{\uparrow}_{toa}\,. \tag{8}$$

Because α is constant, Eq. (8) has the simple solution

$$F^{\uparrow}(h) = F^{\uparrow}_{toa}\left[\frac{\alpha}{2}\,(1-h)+1\right]. \tag{9}$$

With Eq. (5) it follows further from Eq. (9) that

$$F^{\downarrow}(h) = F^{\uparrow}_{toa}\,\frac{\alpha}{2}\,(1-h)\,. \tag{10}$$

Inserting Eqs. (9) and (10) into Eq. (6) leads to the vertical temperature profile of the equilibrated grey atmosphere:

$$T(h) = \sqrt[4]{\frac{F^{\uparrow}_{toa}}{2\,\sigma}\left(\alpha\,(1-h)+1\right)}\,. \tag{11}$$

Evaluating Eq. (9) at the surface ($h = 0$) gives

$$F^{\uparrow}_{toa} = \frac{F^{\uparrow}_{srf}}{\alpha/2+1}\,. \tag{12}$$

Assuming that the surface is a perfect black body for LW radiation, it is

$$F^{\uparrow}_{srf} = \sigma\,T^{4}_{srf}. \tag{13}$$

With Eqs. (12) and (13), the vertical temperature profile described by Eq. (11) can be written as

$$T(h) = T_{srf}\sqrt[4]{\frac{\alpha\,(1-h)+1}{\alpha+2}}\,. \tag{14}$$

Equation (14) implies for the near-surface air that

$$T(0) = T_{srf}\sqrt[4]{\frac{\alpha+1}{\alpha+2}}\,. \tag{15}$$

Hence, $T(0) < T_{srf}$. The reason for this discontinuity at the surface is that, in order to attain the same temperature as the surface, the near-surface air would have to receive as much LW radiation from above as it receives from the surface below, which is not the case (see Eq. (5)). This is a result of the negligence of all mechanisms of energy transfer other than radiation in the model; in reality, the diffusion of heat removes the discontinuity, although sharp temperature gradients right above the surface can still be observed (see for example Pierrehumbert, 2010, whose Eq. (4.45) is identical to our Eq. (15)).

The vertical temperature profile can also be written in terms of the effective radiative temperature of the planet, defined as

$$T_{eff} = \sqrt[4]{\frac{F^{\uparrow}_{toa}}{\sigma}}\,. \tag{16}$$

Inserting T_{eff} into Eq. (11) gives

$$T(h) = T_{eff} \sqrt[4]{\frac{\alpha}{2}(1-h) + \frac{1}{2}}\,. \tag{17}$$

Up to now we have not considered the surface energy balance but determined the vertical temperature profile of an equilibrated grey atmosphere with absorptivity α given an arbitrary surface temperature as lower boundary condition. Equation (14) can thus be interpreted as the *quasi-instantaneous* atmospheric temperature profile. In the following, we consider the situation where not only the atmosphere but also the surface is in thermal equilibrium. We refer to this situation as the overall equilibrium and denote the corresponding variables with the index *eq*.

Assuming that no solar radiation is absorbed within the atmosphere, surface equilibrium requires that

$$S = F^{\uparrow}_{srf,eq} - F^{\downarrow}_{srf,eq}\,, \tag{18}$$

where S is solar radiation absorbed at the surface. Inserting Eq. (5) into Eq. (18) gives

$$S = F^{\uparrow}_{toa,eq}\,, \tag{19}$$

which is the overall equilibrium condition at the top of the atmosphere. It follows with Eq. (16) that

$$T_{eff,eq} = \sqrt[4]{\frac{S}{\sigma}}\,. \tag{20}$$

In overall equilibrium, the vertical temperature profile (Eq. (17)) hence becomes

$$T_{eq}(h) = T_{eff,eq} \sqrt[4]{\frac{\alpha(1-h)+1}{2}}\,. \tag{21}$$

Apart from the different choices of the vertical coordinate, the temperature profile given by Eq. (21) is identical to Eq. (12.21) in Thomas and Stamnes (1999), to Eq. (4.42) in Pierrehumbert (2010), and to Eq. (3.47) in Salby (1992).

Inserting $h = 1$ into our Eq. (21) yields the temperature at the TOA:

$$T_{toa,eq} = T_{eff,eq} \sqrt[4]{\frac{1}{2}}\,. \tag{22}$$

Finally, combining Eqs. (21) and (15) gives the corresponding equilibrium surface temperature:

$$T_{srf,eq} = T_{eff,eq} \sqrt[4]{\frac{\alpha+2}{2}}\,. \tag{23}$$

Equations (21)–(23) reveal that, in overall thermal equilibrium, an increase in absorptivity of a grey atmosphere without non-LW heat sources leads to a temperature increase everywhere except at the TOA where the temperature is independent of α.

Figure 2 shows solutions of Eq. (21) for different values of α. In the limit of an almost completely transparent atmosphere ($\alpha \to 0$), the whole atmosphere attains one single equilibrium temperature (Eq. (22)) and the surface temperature attains the effective equilibrium radiative temperature of the planet (Eq. (20)). Note that the vertically continuous model derived here can be interpreted as a generalization of a discrete-layer model (see Appendix B).

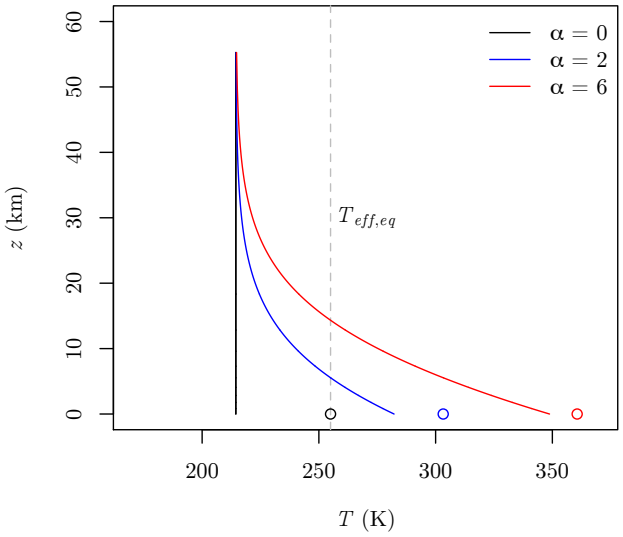

Figure 2. Vertical temperature profiles of a grey atmosphere in overall equilibrium for different absorptivities α. The latter corresponds to α_o in the window-grey model with $\beta_w = 0$. $T_{eff,eq} = 255\,\mathrm{K}$. The circles at $z = 0$ denote the corresponding surface temperatures. Note that the vertical coordinate z is only approximate height, calculated from h with a constant scale height $H = 8\,\mathrm{km}$ such that $h = 1 - e^{-z/H}$.

3 The window-grey atmosphere model

In reality, the atmosphere is not uniformly opaque for LW radiation, as within the grey approximation, but interacts differently with LW radiation of different wavelengths. To account for this in the simplest possible way, we extend the grey model (Sect. 2) by splitting the total LW radiation F into two separate LW bands: an opaque band $F_1 = O$ with opacity $\alpha_o > 0$, and a completely transparent (window) band $F_2 = W$ with opacity $\alpha_w = 0$. With $\beta_w = 1 - \beta_o$ describing the fraction of LW radiation from the surface which is directly emitted to space, the resulting window-grey model has only two parameters: α_o and β_w. Thereby β_w is identical to the so-called transparency factor $\mathcal{G}$ in Thomas and Stamnes (1999), but independent of temperature in our case as we neglect Wien's law. This approach represents the so-called window-grey or one-band Oobleck case of a multiband model (Sagan, 1969; Pierrehumbert, 2010). In contrast to the grey-atmosphere model, the window-grey model allows for the existence of a spectral window, which can be interpreted as an idealisation of the region between 8 μm and 12 μm in the Earth's atmosphere(Fig. 1b). The window-grey model is depicted in Fig. 3.

The window-grey model remains analytically solvable because only radiation in the opaque LW band needs to be considered within the atmosphere. The resulting radiative transfer equation reads

$$\frac{\mathrm{d}O^{\uparrow}(h)}{\mathrm{d}h} = \left[\sigma T(h)^4 (1-\beta_w) - O^{\uparrow}(h)\right] \alpha_o \,, \tag{24}$$

the energy balance equation reads

$$2\,\epsilon_o \sigma T(h)^4 (1-\beta_w) = \epsilon_o \left(O^{\uparrow}(h) + O^{\downarrow}(h)\right), \tag{25}$$

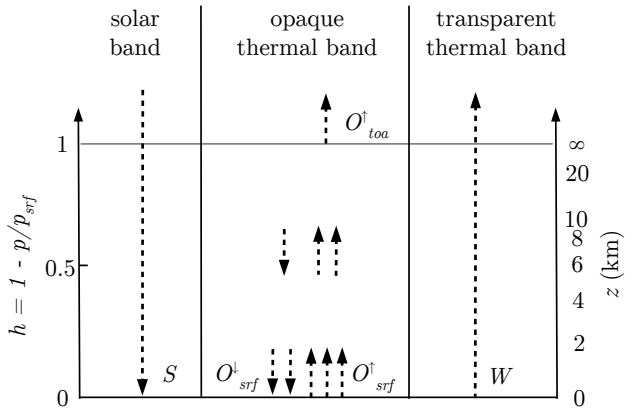

Figure 3. Sketch of the window-grey atmosphere model. S: solar radiation absorbed at the surface. O: radiation in the opaque LW band (↑: upwelling, ↓: downwelling, *srf*: surface, *toa*: top of the atmosphere). W: radiation emitted from the surface in the transparent LW band (atmospheric window). p: pressure. Interpreting the number of arrows in the opaque LW band as proportional to the radiative flux, the illustrated case corresponds to an equilibrated atmosphere with $\alpha_o = 4$.

and the surface emission in the opaque band is

$$O^{\uparrow}_{srf} = (1-\beta_w)\,\sigma\,T^4_{srf}. \tag{26}$$

Equations (24)–(26) can be solved analogously to the corresponding equations describing the grey case (Eqs. (4), (6), and (13)). This leads to the quasi-instantaneous atmospheric temperature profile of the window-grey model. It is

$$T(h) = T_{srf}\sqrt[4]{\frac{\alpha_o\,(1-h)+1}{\alpha_o+2}}\,. \tag{27}$$

Comparison with Eq. (14) reveals that, with the same surface temperature prescribed as lower boundary condition, the vertical temperature profiles in the grey and in the window-grey case are identical for $\alpha_o = \alpha$; the factor $(1-\beta_w)$ in Eqs. (24)–(26) has cancelled.

To determine the overall equilibrium state, the surface energy balance needs to be incorporated. In overall equilibrium it is

$$S + O^{\downarrow}_{srf,eq} = O^{\uparrow}_{srf,eq} + W_{eq} \tag{28}$$

where

$$W_{eq} = \beta_w\,\sigma\,T^4_{srf,eq}\,. \tag{29}$$

Here we omitted the indices denoting the orientation and vertical position of W (as we already did for S) because the only radiation in the window band is the one emitted upward from the surface, and W remains unchanged throughout the atmosphere because $\alpha_w = 0$.

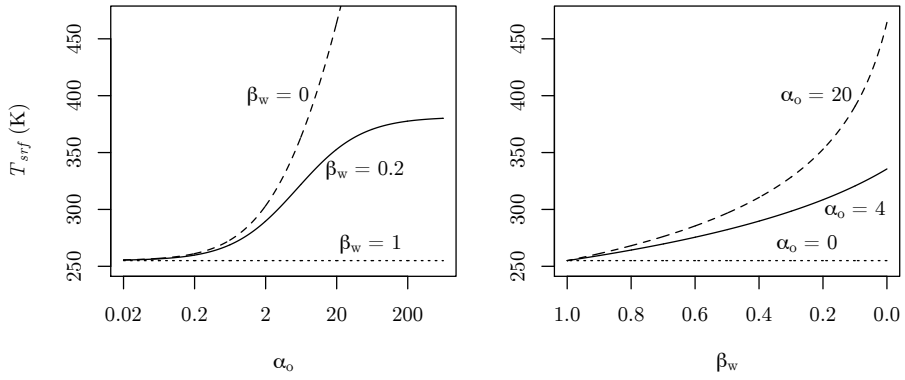

Figure 4. The dependence of the overall equilibrium surface temperature on the parameters α_o and β_w in the window-grey model (Eq. (30)). $\beta_w = 0$ corresponds to the grey case. $T_{\mathit{eff,eq}} = 255\,\mathrm{K}$.

With derivations analogous to the grey case (Sect. 2), one arrives at simple expressions for the overall equilibrium state. The surface temperature for the window-grey model in overall equilibrium is

$$T_{\mathit{srf,eq}} = T_{\mathit{eff,eq}} \sqrt[4]{\frac{\alpha_o + 2}{\alpha_o \beta_w + 2}}\,. \tag{30}$$

The corresponding vertical temperature profile reads

$$T_{\mathit{eq}}(h) = T_{\mathit{eff,eq}} \sqrt[4]{\frac{\alpha_o\,(1-h) + 1}{\alpha_o \beta_w + 2}}\,, \tag{31}$$

which implies for the TOA temperature

$$T_{\mathit{toa,eq}} = T_{\mathit{eff,eq}} \sqrt[4]{\frac{1}{\alpha_o \beta_w + 2}}\,. \tag{32}$$

The TOA temperature, sometimes called the skin temperature (Goody and Yung, 1989; Pierrehumbert, 2010), can be thought of as the temperature an infinitely thin air layer above the atmosphere would have in radiative equilibrium. Obviously, with $\beta_w = 0$ Eqs. (30)–(32) are reduced to the grey case (compare Eqs. (21)–(23)).

Equation (30) implies that an increased absorber amount leads to an increased equilibrium surface temperature (Fig. 4), independent of whether the added molecules absorb in the already opaque part of the LW spectrum (increasing α_o) or in the window region (decreasing β_w, that is, "closing the atmospheric window"). In the following section we discuss the sensitivity of atmospheric temperatures to the model parameters.

4 The mechanisms of CO_2-induced middle-atmosphere cooling

With the window-grey radiation model we are now equipped to investigate the physical essence of CO_2-induced MA cooling. In the window-grey model, the response of temperature to changes in the parameters can be quantified with partial derivatives.

The different effects of CO_2-induced MA cooling can thereby be separated in a formal way. We present such an approach in Appendix C, but constrain the discussion in the following main text largely to the undifferentiated equations.

4.1 The blocking effect

The blocking effect is the result of a change in the long-wave radiative balance when atmospheric CO_2 is increased. Due to the optically thicker atmosphere, less upwelling radiation in the non-window part of the spectrum reaches high altitudes. The temperature at the TOA must thus be lower because, as follows from Eq. (25),

$$T_{toa} = \sqrt[4]{\frac{O^{\uparrow}_{toa}}{2\sigma(1-\beta_w)}}\,. \tag{33}$$

We first investigate the situation in which the assumption of thermal equilibrium is kept for the atmosphere but dropped for the surface. This is a reasonable assumption because the atmosphere adjusts quickly to energetic changes (on the order of months) while the response of the ocean-dominated surface is very slow (including decadal and centennial time scales). In reality, convection closely couples the surface with the troposphere, hence a change in greenhouse gases first affects the middle atmosphere, after which the slow surface-troposphere system adjusts. In the radiation model we represent this time scale separation by letting the atmosphere respond while keeping the surface temperature constant. The temperature profile for this quasi-instantaneous response is given by Eq. (27) which is valid even if the surface is not in thermal equilibrium. Fig. 5 shows the vertical temperature profile before (blue curve) and after (orange curve) increasing α in the grey case (for which α corresponds to α_o with $\beta_w = 0$).

Inserting $h = 1$ in Eq. (27) we arrive at the corresponding quasi-instantaneous TOA temperature:

$$T_{toa} = T_{srf}\sqrt[4]{\frac{1}{\alpha_o + 2}}\,. \tag{34}$$

Equation (34) implies a cooling at the TOA for increased α_o. Furthermore, Eq. (27) implies that at a certain height $\hat{h}_{fast}$ the sign of the fast temperature response due to added greenhouse gases reverses. It is

$$\hat{h}_{fast} = \frac{1}{2}\,. \tag{35}$$

This implies that at first the upper half of the atmosphere (in terms of mass) is cooled while the lower half is warmed.

Both the upper-level cooling and the lower-level warming are due to enhanced blocking, that is, a reduced mean free path of LW radiation in response to increased absorptivity. In equilibrium, the emission, determined by the local temperature, and the absorption of radiation are locally balanced. In the upper atmosphere, where downwelling radiation is subordinate, the upwelling radiation received from below comes from higher (and thus colder) levels when the absorptivity of the atmosphere is increased. Consequently, the air cools until emission and absorption are in balance again. In contrast, in lower levels near the ground, where most of the absorbed upwelling radiation comes directly from the surface (with a fixed temperature), the increased absorptivity mostly affects the downwelling radiation which now comes from lower (and thus warmer) levels, resulting in warming.

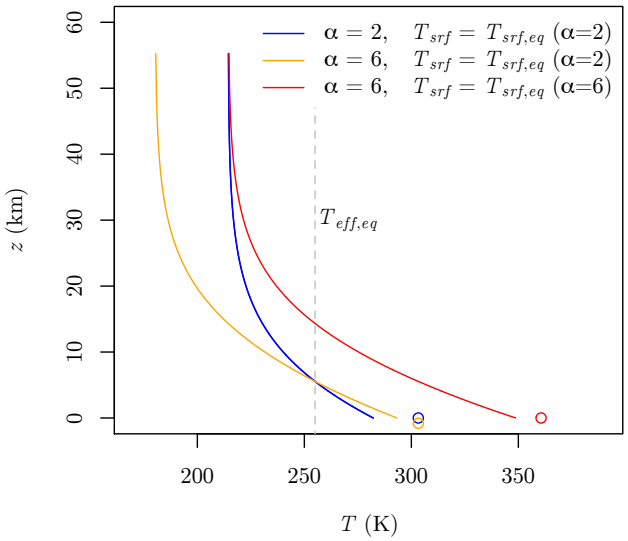

Figure 5. Vertical temperature profiles of a grey atmosphere for two equilibrium states and one transient state. While the blue and red curves show the same equilibria as the corresponding curves in Fig. 2, the orange curve shows the transient state that occurs after switching from $\alpha = 2$ to $\alpha = 6$, directly after equilibration of the atmosphere but with T_{srf} still unchanged. Again α corresponds to α_o in the window-grey model with $\beta_w = 0$. $T_{\mathit{eff}} = 255\,\mathrm{K}$. The circles at $z = 0$ denote the corresponding surface temperatures. Note that the vertical coordinate z is only approximate height, calculated from h with a constant scale height $H = 8\,\mathrm{km}$ such that $h = 1 - e^{-z/H}$.

As long as the emission from the surface, determined by its temperature, remains unchanged, the surface energy budget is imbalanced due to the increased downwelling radiation. The surface will thus warm – which is the common greenhouse effect – until a new overall equilibrium is attained. During the gradual ascent of the surface temperature, accompanied by increasing upwelling radiation, the whole atmosphere warms (Eq. 27), and the height at which the sign of the temperature change reverses is shifted upwards. In the grey case, where $\beta_w = 0$, this shift proceeds until the whole atmosphere except the TOA is warmer than originally (red curve in Fig. 5). The upper-level cooling in response to increased absorptivity in a grey atmosphere (and without absorption of solar radiation within the atmosphere) is thus only a transient effect that vanishes when the new overall equilibrium is reached. This is a consequence of the outgoing longwave radiation (OLR) having to balance S, which is constant in the model. Even in the very simple grey model a solar and a greenhouse forcing act differently: While an increase in S would force the OLR to increase as well, the OLR does not change when CO_2 is increased, even though the temperature is increased throughout the atmosphere.

The situation is different in the presence of an atmospheric window where a part of the surface radiation is emitted directly to space, bypassing the atmosphere. An atmospheric window implies a reduced sensitivity of the surface temperature to the state of the atmosphere (its absorptivity in the opaque band and the corresponding temperature profile, see Eq. (30)) because the radiation in the opaque LW band becomes less important in the surface energy budget (Eq. (28)) with increasing window

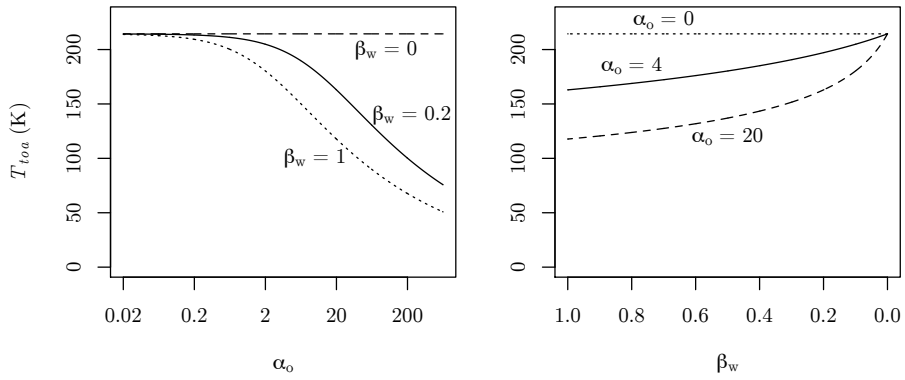

Figure 6. The dependence of the overall equilibrium temperature at the top of the atmosphere on the parameters α_o and β_w in the window-grey model (Eq. (32)). $\beta_w = 0$ corresponds to the grey case. $T_{eff,eq} = 255\,\mathrm{K}$.

size. Consequently, in the presence of an atmospheric window, a permanent cooling at the TOA remains after the surface has equilibrated (Eq. (32)).

It becomes evident from Eq. (32) that, in contrast to the surface, at the TOA the sign of the temperature response depends on the spectral property of the added absorbers: if they absorb in the already opaque part of the LW spectrum (increasing α_o), $T_{toa,eq}$ is decreased (MA cooling), but if they absorb in the transparent part of the LW spectrum (decreasing β_w, that is, "closing the atmospheric window"), $T_{toa,eq}$ is increased (MA warming) (Fig. 6).

In fact, decreasing β_w leads in overall equilibrium to a temperature increase at every height in the atmosphere (Fig. 7, top). In contrast, if molecules absorbing in the opaque LW band are added, the sign of the equilibrium temperature response reverses at a certain height $\hat{h}_{eq}$, with cooling above and warming below (see Eq. (C6); Fig. 7 bottom):

$$\hat{h}_{eq}(\beta_w) = 1 - \frac{\beta_w}{2}\,. \tag{36}$$

For $\beta_w = 0$, that is in the grey case, $\hat{h}_{eq}$ becomes 1 (the corresponding geometric height $\hat{z}_{eq}$ becomes ∞), meaning that no cooling takes place.

We term the above described cooling in the upper parts of the atmosphere the *blocking effect* of CO_2-induced MA cooling. This presupposes that the main consequence of adding CO_2 to the atmosphere is, in terms of the window-grey model, an increase of α_o rather than a decrease of β_w. The permanent component of this effect, the *permanent blocking effect*, is revealed by Eqs. (31) and (32). It has to be distinguished from the instantaneous blocking effect, which consists of the permanent blocking effect and a transient component. The instantaneous blocking effect can be observed when atmospheric CO_2 is altered but when the surface temperature has not yet adjusted to the forcing (which is to some extent also the case for present-day Earth). In the grey model the blocking effect is only a transient phenomenon: the entire atmosphere has warmed (except at the TOA) after the surface has equilibrated. In the window-grey model the blocking effect has a permanent component that persists after the surface has adjusted.

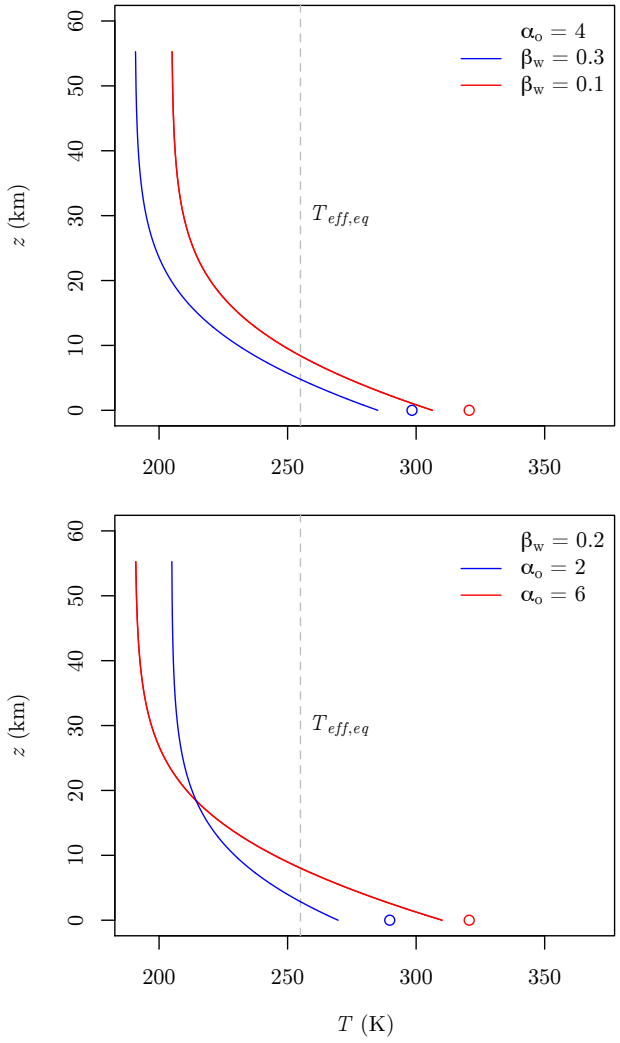

Figure 7. Vertical temperature profiles in overall equilibrium for the window-grey case with $T_{eff,eq} = 255\,\mathrm{K}$ for different combinations of the parameters α_o and β_w (Eq. (31)). The circles at $z = 0$ denote the corresponding surface temperatures. Note that the vertical coordinate z is only approximate height, calculated from h with a constant scale height $H = 8\,\mathrm{km}$ such that $h = 1 - e^{-z/H}$.

The blocking effect can be understood in terms of the interplay between the sensitivity of the surface temperature to greenhouse-gases on the one hand and the blocking of upwelling LW radiation by greenhouse gases on the other hand: while an atmospheric window diminishes the sensitivity of the surface temperature to α_o (see Eq. (30)), the blocking associated with α_o is independent of the presence or width of an atmospheric window (see Eq. (27)). Only in the grey case, where the sensitivity of the surface temperature is at its maximum (Eq. (30)), the surface temperature response is strong enough to compensate for the blocking effect, resulting in an α_o-independent equilibrium TOA temperature (compare Eq. (32)).

Another way of looking at the permanent blocking effect goes via the emission spectrum of the planet viewed from space (i.e., the upwelling LW radiation at the TOA). If the surface warms in response to an increased α_o, the radiation in the window region of the spectrum W will be accordingly stronger, corresponding to a Planck curve at the increased surface temperature. In overall equilibrium the radiation in the opaque band $O^{\uparrow}_{toa}$ must be shifted to lower intensity to compensate for W, given that the solar energy input is unchanged. It then follows from Eq. (33) that the temperature at the TOA must decrease. The same argument reveals why the TOA cooling due to enhanced blocking in a grey atmosphere can only be a transient phenomenon: If no window exists, $O^{\uparrow}_{toa}$ must attain its original intensity after equilibration to balance the unchanged solar energy input.

4.2 The indirect solar effect

On Earth not all solar radiation transects the air unhindered, but some is absorbed within the atmosphere and leads to increased temperatures, particularly in the upper parts of the ozone layer. The solar heating can be incorporated into Eq. (25) as an additional term $S^*(h)$:

$$2\,\epsilon_o\,\sigma\,T^*(h)^4(1-\beta_w) = \epsilon_o\,\left(O^{\uparrow}(h)+O^{\downarrow}(h)\right) + S^*(h)\,. \tag{37}$$

Eq. (37) is similar to Eq. (6.15) in Neelin (2011), except that Neelin considers only the grey case ($\beta_w = 0$) and neglects the downwelling LW radiation, constraining the validity of the equation to the vicinity of the TOA.

Assuming that solar heating is confined to an infinitesimally thin layer at $h = h'$, such that the equilibrium temperature everywhere else remains unchanged and, thus, $O^{\uparrow}(h')$ and $O^{\downarrow}(h')$ are not affected by the additional term, one arrives at

$$T^*(h')^4 = T(h')^4 + \frac{s^*(h')}{\alpha_o(1-\beta_w)}\,, \tag{38}$$

where $T(h')$ is the solution of Eq. (37) with $S^*(h') = 0$, that is, the window-grey solution of Eq. (25), and $s^*(h') = S^*(h')/(2\,\sigma\,\mathrm{d}h)$.

Equation (38) reveals the following: Given that due to an additional term in the local energy budget the atmospheric temperature at some height is deflected from the window-grey solution, increasing the amount of LW absorbers in the atmosphere results in a relaxation of the temperature towards the window-grey solution. This holds both for increasing α_o and for decreasing β_w. It must be kept in mind though that the window-grey solution itself depends on α_o and β_w (Eq. (31)), making the relaxation towards the window-grey solution an additional effect. Figure 8 illustrates the indirect solar effect for the grey case (i.e., for $\beta_w = 0$).

If the additional term s^* is positive, as it is the case for the absorption of solar radiation by ozone, increasing the emissivity either by increasing α_o or by decreasing β_w results in local cooling. We call this effect the *indirect solar effect* of CO_2-induced MA cooling. The term "indirect" reminds us that this effect is not due to any change in solar heating rates as might be caused by a change in ozone concentrations. Instead, the mere presence of solar absorption is a prerequisite for this effect. Like the permanent blocking effect, the indirect solar effect is still at work when the system has reached the new (more opaque) overall equilibrium. Note that the indirect solar effect would also manifest if the opacity was changed only locally. This is not the case for the blocking effect, where integration over a finite layer with perturbed opacity is needed.

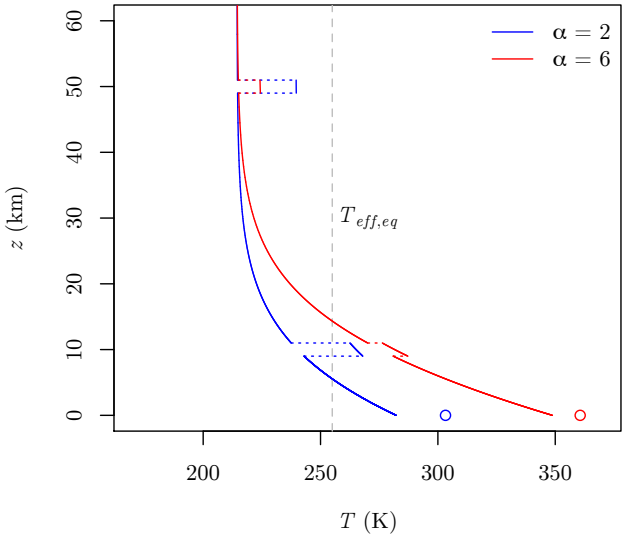

Figure 8. Vertical temperature profiles of a grey atmosphere that is additionally locally heated (e.g., by absorption of solar radiation) at two heights within the atmosphere. Apart from the heights at which the profiles are locally deflected due to additional heating, the blue and red curves show the same grey equilibria as the corresponding curves in Fig. 2. Again α corresponds to α_o in the window-grey model with $\beta_w = 0$. The heights at which additional heating occurs ($z_1 \approx 10\,\mathrm{km}$, $z_2 \approx 50\,\mathrm{km}$) and the magnitude of the additional heating terms (specified such that the temperature rise is $25\,\mathrm{K}$ for $\alpha = 2$ at both heights) are more or less arbitrarily chosen to demonstrate the effect. $T_{\mathit{eff,eq}} = 255\,\mathrm{K}$. The circles at $z = 0$ denote the corresponding surface temperatures. Note that the vertical coordinate z is only approximate height, calculated from h with a constant scale height $H = 8\,\mathrm{km}$ such that $h = 1 - e^{-z/H}$.

5 Effect strengths

An essential question so far unanswered is how strong the above derived effects are compared to each other. In this section we apply a complex atmospheric model to give a quantitative answer to this question, and we discuss the implications and limitations of the window-grey model in the light of these results.

5.1 Simulations with a complex atmospheric model

To complement the findings obtained with the window-grey model, and to derive meaningful estimates for the strength of the effects, we have conducted simulations with the complex atmospheric general circulation model ECHAM6 (Stevens et al., 2013). This model and its predecessors have been used for comprehensive simulations, including future climate projections, in the different phases of the Coupled Model Intercomparison Project (CMIP), which are the backbone of the reports compiled by the Intergovernmental Panel on Climate Chance (IPCC). These models, including ECHAM6, therefore have sophisticated parameterizations for, e.g., radiation, convection, clouds, boundary-layer turbulence, and gravity waves, and numerically solve the governing equations of fluid dynamics on grids with steadily increasing spatio-temporal resolution. The radiative trans-

Table 1. ECHAM6 simulations

Simulation ID	Solar absorption in the atmosphere	SST treatment	CO_2[a]	CFC-11 /-12[b]	GMST[c] [K]	OLR[d] [W/m^2]	planetary albedo [%]
REF	yes	free equilibration	1x	1x	287.14	241.41	29.03
CO_2x2	yes	free equilibration	2x	1x	289.36	241.58	29.00
CO_2x2_{fixSST}	yes	prescribed from REF	2x	1x	287.41	238.11	28.91
$CFCx15$	yes	free equilibration	1x	15x	288.97	241.96	28.89
$CFCx15_{\text{fixSST}}$	yes	prescribed from REF	1x	15x	287.29	238.88	28.80
REF_{ns}	no	free equilibration	1x	1x	286.09	227.43	33.08
CO_2x2_{ns}	no	free equilibration	2x	1x	288.31	227.52	33.03
$CFCx15_{\text{ns}}$	no	free equilibration	1x	15x	287.88	227.56	33.05

[a] 1x: CO_2=280ppmv; 2x: CO_2=560ppmv

[b] 1x: CFC11=0.2528ppbv, CFC12=0.4662ppbv; 15x: CFC11=3.792ppbv, CFC12=6.993ppbv

[c] global annual-mean near-surface air temperature

[d] outgoing longwave radiation at the top of the atmosphere

fer scheme used in ECHAM6, which employs 16 LW bands, has been shown to give instantaneous clear-sky responses to greenhouse-gas perturbations in close agreement with accurate line-by-line calculations (Iacono et al., 2008). To adequately resolve the middle atmosphere, we have used the T63L95 configuration with relatively coarse ($\sim 2^\circ$) horizontal but high (95 levels, top at 0.01 hPa) vertical resolution. The distribution of ozone is prescribed by a climatology.

The ocean and sea ice have been treated in a simple way similar to the approach of Dickinson et al. (1978). The ocean surface temperature and sea ice concentration and thickness are prescribed with a realistic seasonal and spatial pattern derived from observations. After every year the ocean surface temperature pattern is updated uniformly according to the total energy imbalance integrated over the global ocean surface (including sea ice) and over the year, using a heat capacity that corresponds to a 50 m thick mixed-layer ocean. Despite changing temperatures, the sea ice state pattern is not updated, leading to discrepancies between the sea ice and ocean states. This procedure also suppresses further changes to the surface temperature pattern, such as polar warming amplification. However, this allows for a rapid thermal equilibration of the surface with an exponential timescale of $\sim$3 years, serving the purpose of this paper where the focus is on the global-mean response.

We have conducted eight ECHAM6 simulations with differences in (i) the treatment of solar radiation, (ii) the treatment of sea-surface temperatures (SST), and (iii) the abundance of greenhouse gases (Tab. 1). In five simulations the solar radiation follows the default behavior, with some of the solar radiation absorbed by gases within the atmosphere. This set includes one reference simulation where pre-industrial greenhouse-gas concentrations are used and the SSTs are allowed to run into equilibrium, and four sensitivity simulations. In two of these the ocean is allowed to attain a new equilibrium, either with the CO_2 concentration doubled or with the Chlorofluorocarbon (CFC-11 and CFC-12) concentrations increased by the factor 15,

chosen such that the surface warming is similar compared to the case of CO_2 doubling. The other two sensitivity simulations are identical with the previous two, except that the SSTs are prescribed from the reference simulation.

In another set of three simulations the absorption of solar radiation by all atmospheric gases (but not cloud droplets or ice) is turned off. This set also includes a reference simulation and two sensitivity simulations with increased CO_2 and CFC concentrations. In these, the SSTs are again allowed to run into equilibrium. All simulations are conducted over 22 years, but only the last 10 years are used to compute averages for the analysis because it takes a few years (in our setup) until an equilibrium is reached. This experimental design allows us first to demonstrate the dependence of MA temperature changes on the spectral properties of the added absorbers: CFCs absorb mainly in the spectral window of the Earth's atmosphere, whereas CO_2 absorbs mainly at wavelengths where the atmosphere is already relatively opaque. Second, we can quantify the effect strength for the two permanent effects by which CO_2 cools the MA, deduced above with the window-grey model, and investigate how atmospheric temperatures respond to the slow surface adjustment.

When the absorption of solar radiation by gases is switched off, the total short-wave absorption in the atmosphere drops from 75 W/m^2 in REF to only 13 W/m^2 in REF$_{ns}$, the residue being due to absorption by tropospheric clouds. The lack of short-wave heating due to ozone leads to a strong cooling of the MA. The local temperature maximum around the stratopause completely disappears and temperatures drop to $\sim$160 K in the upper stratosphere and in the mesosphere, in agreement with previous studies (Manabe and Strickler, 1964; Fels et al., 1980). Tropospheric temperatures are only slightly reduced by $\sim$1 K (Tab. 1 and Fig. 9 left). This small temperature change is the result of a compensation of different effects. After removing the absorption of solar radiation, more short-wave radiation propagates downwards through the atmosphere. A part of the previously absorbed radiation is then scattered and the planetary albedo increases from 29 % to 33 %. The rest is partly absorbed in the troposphere by cloud droplets and ice crystals, and partly reaches the Earth's surface where the downwelling solar radiation is increased by 42 W/m^2. This instantaneous redistribution of short-wave fluxes tends to warm the surface. However, the large cooling in the MA that follows also leads to a decreased downwelling long-wave radiation at the surface which has a cooling effect. To this extent, our result is in line with previous simulations that quantified the effects of stratospheric ozone removal (Ramaswamy et al., 1992; Hansen et al., 1997; Forster et al., 1997a; Stuber et al., 2001). In contrast to these studies, we still keep ozone as a greenhouse gas as only its short-wave absorption is removed. However, this is not a very important difference as the short-wave effect of ozone has been shown to be more important than the long-wave effect (Dickinson et al., 1978; Ramaswamy et al., 1992; Forster et al., 1997a). A similar cancellation of short- and long-wave effects on the surface temperature seems to hold for other gases. The lack of absorption by water vapour further shifts the heating from the lower troposphere to the surface, without much impact on the surface temperature. An additional effect that might be of relevance for the surface cooling in these simulations is the reduction in specific humidity due to the atmospheric cooling.

Our simulations with perturbations in CO_2 and CFCs are in the tradition of several pioneering studies on the role of greenhouse gases (Manabe and Strickler, 1964; Manabe and Wetherald, 1967, 1975; Dickinson et al., 1978; Fels et al., 1980), and confirm their results. With standard treatment of solar radiation, CO_2 doubling in ECHAM6 leads to an increase in global annual-mean near-surface temperature by 2.2 K; this is the climate sensitivity of our model setup. The tropospheric warming in fact increases with height, reaching a maximum of 3.5 K in the upper troposphere (Fig. 9 middle, red solid curve). This pattern,

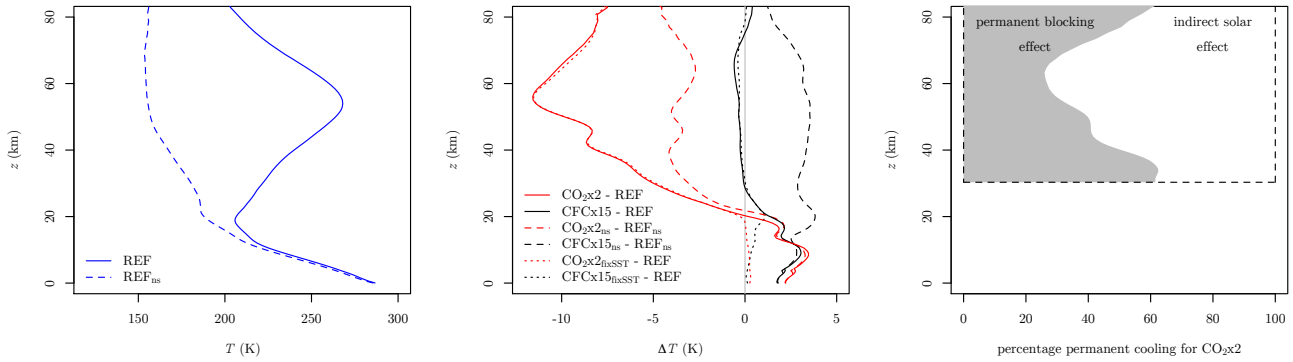

Figure 9. Results obtained with ECHAM6 coupled to a simplistic ocean model to allow for rapid thermal adjustment of the surface. Left: Global annual-mean equilibrium temperature profiles for two reference runs under pre-industrial external forcing, with (solid; REF) and without (dashed; $\mathrm{REF_{ns}}$) absorption of solar radiation in the atmosphere. Middle: Temperature difference to the corresponding reference runs in response to increased CO_2 or CFC concentrations (simulation IDs are explained in Tab. 1). Right: Percentage of the permanent cooling effect in response to CO_2 doubling from the window and indirect solar effects, estimated by dividing $\mathrm{CO_2}x2_{\mathrm{ns}} - \mathrm{REF_{ns}}$ by $\mathrm{CO_2}x2 - \mathrm{REF}$. Note that the vertical coordinate z is only approximate height, calculated from h with a constant scale height $H = 8\,\mathrm{km}$ such that $h = 1 - e^{-z/H}$.

which is not captured by the window-grey model, results from the temperature dependence of the moist-adiabatic lapse rate (the so-called lapse-rate feedback) and is thus related to convective processes. Somewhat above the tropopause the temperature response changes sign. In agreement with earlier studies (Manabe and Wetherald, 1967; Fels et al., 1980), the cooling then increases with height and assumes a maximum cooling by 11.6 K around the stratopause region.

Adding CFCs instead of CO_2 results (by design) in a similar tropospheric response with a near-surface warming by 1.8 K, but temperatures in the MA remain virtually unchanged (Fig. 9 middle, black solid curve). Again, this result agrees with previous studies (Dickinson et al., 1978; Forster and Joshi, 2005). However, our simulations also show that the near-zero MA temperature change is due to a cancellation of two effects: The indirect solar effect is not wavelength dependent. More absorbers increase emission more strongly than they increase absorption, thereby reducing the relative importance of the solar heating term (Sect. 4.2). This suggests that another effect counteracts the cooling from the indirect solar effect. The above considerations based on the window-grey model suggest that this counteracting warming effect can be interpreted as an *inverse blocking effect*: Instead of making the already opaque part of the spectrum even more opaque, which mainly happens when CO_2 is added, the increase of CFC concentrations acts to narrow the atmospheric window, corresponding to a decrease of β_w in the window-grey model (Figs. 7 and 6 top). In fact, the situation corresponds not only to a decrease of β_w, but also to a simultaneous decrease of α_o because the average opacity of what should be translated into the single opaque band of the window-grey model is decreased by the inclusion of the CFC-affected – still relatively transparent – parts of the previous window band. Overall, the MA is more strongly subjected to the radiation from the warm surface.

In the case without solar absorption by gases within the atmosphere, adding CO_2 or CFCs results in similar responses in the troposphere, but markedly different responses in the MA (Fig. 9 middle, dashed curves): While the cooling in response to CO_2 is roughly halved, the previously neutral response to CFCs turns into a substantial warming by up to 3.5 K. These results are consistent with the interpretation that the cooling due to the indirect solar effect has been precluded, leaving only the response due to the blocking effect (in the CO_2 case) and the inverse blocking effect (in the CFC case).

Under the assumption of linearity, this allows us to estimate the fractional contributions of the two permanent effects to MA cooling (Fig. 9 right). According to our results the indirect solar effect contributes up to $\sim$70 % to the total permanent cooling around the stratopause where solar heating is strongest. Outside this region the blocking effect gains importance and begins to dominate the cooling in the middle stratosphere and the middle mesosphere. The assumption of linearity is rather crude, so these estimates should be taken with a grain of salt. In fact, it is probably not possible to make a completely clean quantitative distinction, as the formal analysis in Appendix C3 suggests.

The window-grey model also suggests a transient MA cooling that adds to the permanent cooling before the surface temperature has adjusted to the changed radiative forcing. We can investigate this effect with the remaining two simulations where the greenhouse gases are perturbed but SSTs are fixed to the reference state (Tab. 1). Interestingly, the initial MA responses (Fig. 9 middle, dotted curves) are nearly identical with the corresponding equilibrium responses (solid curves) above $\sim$20 km. This means that, given a fixed atmospheric composition in terms of well-mixed greenhouse gases, MA temperatures are almost independent of the surface temperature.

In the window-grey model the increased surface temperature entails increased upwelling LW radiation in both the window and the opaque band. In contrast, the additional upwelling LW radiation of approx. 3.5 W/m^2 (beyond the tropopause) in CO_2x2 compared to CO_2x2_{fixSST} is constrained to transparent parts of the spectrum and has thus no impact on MA temperatures. This result is not specific to our simulations and in line with previous studies. In particular, Forster et al. (1997b) use a radiative-convective model and show that the radiative forcing by CO_2 depends on the definition of the tropopause. While this affects the response of the surface-troposphere system, the temperature profile above is not affected by the definition of the tropopause (see their Fig. 8a). A similar argumentation applies to changes in surface albedo: The latter would affect the surface temperature directly and lead to an adjustment of the troposphere, but the effect decays with height (Manabe and Wetherald (1967), Fig. 19). Hence, the temperature in the MA appears to be directly determined by the actual atmospheric composition and not by the history of this composition (i.e., the concentration scenario) and associated surface temperature changes.

A possible explanation for the discrepancy between complex models and the window-grey model regarding the slow MA adjustment, as well as other limitations of the window-grey model are discussed in the following section.

5.2 Limitations of the window-grey model

Given the simplicity of the window-grey model, quantitative statements are difficult to make and the cases shown in Figs. 2, 5, 7, and 8 are quantitatively unrealistic. Here we nevertheless attempt to derive some crude estimates based on the window-grey model, and discuss discrepancies to ECHAM6 in the light of obvious limitations of the window-grey model.

First we investigate the strength of the permanent blocking effect at the TOA in relation to the surface response. It follows from Eqs. (30) and (32) that

$$\frac{\partial T_{toa,eq}}{\partial \alpha_o} / \frac{\partial T_{srf,eq}}{\partial \alpha_o} = -\frac{1}{2} \left(\frac{T_{srf,eq}}{T_{toa,eq}} \right)^3 \frac{\beta_w}{1-\beta_w} \,. \tag{39}$$

One can now insert typical temperatures prevailing at the Earth's surface ($\sim$290 K) and at the mesopause ($\sim$180 K), and an estimate of $\beta_w \approx 10-20\,\%$ (the actual values depend on the optical thickness threshold used to derive β_w from the continuous absorption spectra, compare Fig. 1b-c). This simple calculation yields response ratios of approximately only $(-0.2)-(-0.5)$, i.e., a larger temperature change at the surface than in the MA. This result stands in sharp contrast to ECHAM6 where the surface warms much more than the MA cools by the permanent blocking effect.

Probably the main reason for this discrepancy is that the effective width of the atmospheric window is very different for the atmosphere as a whole and for the atmosphere beyond the tropopause alone. The width of the atmospheric window is however crucial for the atmospheric temperature profile and the strength of the MA cooling effects both in absolute and relative terms. Considering that $\beta_w \approx 90-95\,\%$ is more representative for the largely water-free atmosphere beyond the tropopause (compare Fig. 1), Eq. (39) yields a response ratio of $(-20)-(-40)$, which is in much better agreement with the ECHAM6 results.

Regarding the transient component of the MA cooling, the window-grey model predicts that the transient temperature adjustment decays with height (see also Appendix C2, Eq. (C10)), but it fails to explain the virtual absence of a transient MA adjustment in ECHAM6. This might be linked to another effect neglected in the window-grey model, namely the water vapor feedback. Higher tropospheric temperatures imply higher water vapour concentrations, leading to a pronounced temperature dependence of the atmospheric opacity. The increased opacity as a result of tropospheric warming entails that a *secondary blocking effect* may counteract the slow reduction of the initial MA cooling associated with the transient component of the blocking effect seen in the window-grey model. We therefore speculate that the water vapour feedback might play a role to explain the apparent insensitivity of MA temperatures to the surface temperature by redirecting changes in upwelling LW radiation to parts of the spectrum that are transparent in the MA.

Moreover, the height-dependent width of the atmospheric window acts in concert with the effect of convection. Convection acts to reduce the lapse rate considerably, to $\sim$6.5 K/km in the current climate, leading to an approximately constant lapse rate in the troposphere (e.g., Manabe and Wetherald, 1967). The appearing radiative-convective equilibrium in the troposphere is associated with an upward heat transport and increased temperatures in the free troposphere and decreased temperatures at (and close to) the surface. The redistribution of heat from the surface to the upper troposphere by convection thus bypasses the lower levels where the atmospheric window is small. Tropospheric convection is thus an efficient process to attenuate the surface response to greenhouse forcing, but convection is neglected in the window-grey model.

It is tempting to apply the window-grey model only to the MA, prescribing the upward radiative flux in the opaque thermal band ($O^{\uparrow}$) at the tropopause as a lower boundary condition. The omission of the troposphere would have the advantages that convection does not play a significant role anymore and that the complex influence of the unevenly distributed atmospheric water (in all its aggregate phases) is strongly diminished.

A way to achieve this for the grey model is to apply Eq. (9) at the tropopause (index *tp*) and to insert it into Eq. 11. Transferred to the window-grey model, this yields

$$T(h) = \sqrt[4]{\frac{O_{tp}^{\uparrow}}{\sigma\,(1-\beta_w)}\,\frac{\left(\alpha_o\,(1-h)+1\right)}{\left(\alpha_o\,(1-h_{tp})+2\right)}}\,. \tag{40}$$

One could now investigate how changes in $O_{tp}^{\uparrow}$ or h_{tp} affect the MA, but this would not be very conclusive because $O_{tp}^{\uparrow}$ and h_{tp} respond in a complex manner to changes in greenhouse-gas forcing. One could also follow a hybrid approach by using values derived from a complex model like ECHAM6 for $O_{tp}^{\uparrow}$ and h_{tp}. However, in particular the derivation of $O_{tp}^{\uparrow}$ from a multi-band LW scheme would not be straight forward. Moreover, the ECHAM6 results show that above a certain height the temperature profile will not respond to changes in the troposphere. In other words, $O_{tp}^{\uparrow}$ and h_{tp} appear to change in such a way that the temperature profile above remains the same. Overall, applying the window-grey model only to the MA appears not to add to our explanation of why CO_2 cools the MA.

6 Summary and conclusions

In this article we explain a well-known phenomenon that is central to our general understanding of climate change – cooling of the middle atmosphere (MA) by CO_2 – in a simple but physically consistent way. We do so by applying a vertically continuous window-grey radiation model to the phenomenon. This way it is possible to distinguish two main effects by which CO_2 cools the MA.

First, enhanced blocking of upwelling LW radiation operates towards lower MA temperatures. In principle, this *blocking effect* has a transient component due to the slow warming of the surface. This adjustment leads to intensified upwelling LW radiation and tends to reduce the initial MA cooling in the window-grey model. While these effects exactly compensate each other in a grey atmosphere, leading to an equilibrium TOA temperature that is independent of the atmospheric opacity, the blocking of upwelling LW radiation outweighs in the presence of a spectral window because of the reduced surface temperature sensitivity, leaving lower equilibrium temperatures above a critical height after the adjustment. Hence, the blocking effect is permanent because the Earth's atmosphere is not grey, i.e., uniformly opaque for LW radiation at any wavelength, but absorbs and emits LW radiation with varying intensity depending on wavelength. The introduction of a spectral window into an otherwise uniformly opaque atmosphere is the simplest possible means to capture the effect in a physical model.

The second permanent effect of CO_2-induced MA cooling is the *indirect solar effect*. It owes its existence to the fact that there are heat sources within the atmosphere in addition to LW radiation, most importantly solar radiation that is absorbed in particular in the vicinity of the stratopause by ozone. The additional heating term causes a deviation of the temperature profile from the window-grey solution. The strength of this deviation depends on the abundance of LW absorbers because the relative importance of the constant additional heating term in the local energy budget decreases with increasing LW absorber abundance.

While the window-grey model allows for a fully analytical treatment of CO_2-induced MA cooling, it is not well suited to constrain the relative effect strengths. Uncertainties are large because the window-grey model entails a number of gross

simplifications, including in particular: the assumption of vertically well-mixed greenhouse gases (violated in particular by water vapour); the simplistic LW band structure; and the neglect of vertical heat transport by convection (and conduction at the surface). Additional simplifications are: the neglect of Wien's law; the two-stream approximation; the neglect of the horizontal dimensions and the associated differential heating and atmospheric dynamics (including gravity waves); the neglect of chemical processes; the implicit treatment of solar radiation; the neglect of clouds, aerosols, and scattering in general; and the assumption of local thermodynamic equilibrium that does not hold in the upper mesosphere and beyond. Most of these factors are discussed for example in Pierrehumbert (2010), and those specific to the mesosphere are reviewed in Mlynczak (2000).

Therefore, to quantify the effect strengths and to complement the insights gained from the window-grey model, we have conducted simulations with a much more complex atmospheric model. The results indicate that the two permanent effects are similarly important, with the indirect solar effect dominating around the stratopause and the blocking effect dominating away from the stratopause. The window-grey model also predicts a slow (re-)warming throughout the atmosphere in response to the slow surface warming. However, this transient effect is negligible in the MA according to the simulations with the complex model, pointing to the limitations of the window-grey model.

This article is meant to consolidate our understanding of why CO_2 cools the middle atmosphere by filling a gap between reality and complex atmospheric models on the one side and somewhat scattered heuristic arguments on the other. The reconsideration of CO_2-induced MA cooling as put forward here has a distinct educational element, with the potential to convey the physical essence of the involved mechanisms to a broader audience.

Appendix A: An analogy for the blocking effect

While the explanations based on the window-grey model involve mathematical formalism, the following analogy may facilitate an intuitive understanding for the permanent and transient components of the blocking effect.

Consider a building that is heated at a constant rate from inside. In steady state there is a higher temperature inside the building compared to the fixed exterior temperature. The walls of the building represent an analogy to the Earth's atmosphere, with the outer surface as the top of the atmosphere and the inner surface as the atmosphere close to the Earth's surface. The temperature at the outer wall surface is higher than the exterior temperature and the temperature at the inner wall surface is somewhat lower than the interior (room) temperature. These temperature differences maintain an export of heat at the same rate at which the interior is heated. In the following we assume that the walls have negligible heat capacity whereas the interior reacts more inertly to disturbances due to a non-zero heat capacity.

We first assume that the building is insulated equally well everywhere (corresponding to the grey case), resulting in a uniform temperature of the outer surface. If now the heat resistance of the walls is instantaneously increased, at first the outer surface temperature drops and the inner surface temperature rises, while the interior temperature is still unchanged. In this situation less heat escapes from the building than is released by the heating system. The imbalance leads to a slow ascent of the interior temperature that continues until the outer surface temperature returns to its original value. The initial cooling of the outer

surface temperature is analogous to the quasi-instantaneous cooling that occurs in the upper half of the atmosphere in the grey model; the cooling is only transient and has no permanent component.

Assuming instead that there are parts of the building envelope that are more weakly insulated than the remainder, as is typically the case with windows, the outer surface temperature in equilibrium is higher at the windows than it is at the walls, and a larger fraction of the total energy escapes via the windows compared to how much they contribute to the total area of the building envelope. If now the heat resistance of the walls is increased, the outer surface temperature of the wall is diminished not only temporarily, but some cooling remains also after the interior temperature has increased to its new equilibrium value. In the new equilibrium, even more energy escapes through the windows and less through the walls. The permanent cooling of the outer surface temperature of the walls is analogous to the cooling in the higher atmosphere associated with the permanent blocking effect of CO_2-induced MA cooling.

The main difference between the building analogy and the window-grey radiation model is that the separation between walls and windows in the former case is in geometrical space, whereas the separation into an opaque and a transparent radiation band in the latter case is in spectral space. Another obvious difference is that the mechanism of energy transfer is heat conduction in the walls of a building as opposed to radiation in the atmosphere. Nevertheless, we reckon the analogy of an insulated building as a valid means to illustrate the blocking effect of CO_2-induced MA cooling.

Appendix B: Relation to discrete-layer models

Without showing derivations we point out that the vertically continuous model(s) presented in the main text can be interpreted as a generalization of discrete-layer models. The simplest type of the latter, a model with only one grey atmospheric layer, is widely used to explain the greenhouse effect in a conceptual way (e.g., Pierrehumbert, 2010; Neelin, 2011). In the following we discuss only the grey case, but the window-grey case can be treated analogously.

In an n-layer grey-atmosphere model with uniform layer emissivity ϵ_l, from the radiative balances at every atmospheric layer it follows that, given an arbitrary surface temperature, the equilibrium temperature at layer i is

$$T_i = T_{srf} \sqrt[4]{\frac{\epsilon_l\,(n-i)+1}{\epsilon_l\,(n-1)+2}} \tag{B1}$$

where $i = 1$ is the lowest and $i = n$ the highest atmospheric layer. The overall equilibrium situation is obtained when T_{srf} in Eq. (B1) is replaced by the value it attains in overall equilibrium, which is

$$T_{srf,eq} = T_{eff,eq} \sqrt[4]{1 + \frac{n\,\epsilon_l}{2-\epsilon_l}}\,. \tag{B2}$$

For $\alpha/2 \in \mathbb{N}$ the vertically continuous grey model is equivalent to a discrete grey model with $n = \alpha/2$ atmospheric layers, each with emissivity $\epsilon_l = 1$. The heights h that correspond to the discrete levels i are then determined by

$$h_i = \frac{i - \frac{1}{2}}{n}\,. \tag{B3}$$

Although providing a very suitable conceptual tool to understand the greenhouse effect, the discrete-layer grey-atmosphere model (just like its continuous analogue) obviously can not explain greenhouse-gas induced MA cooling. For such an explanation it is again necessary either to introduce non-uniform opacity for LW radiation (e.g., by introducing an atmospheric window), or to introduce an additional (solar) heating term.

Appendix C: Formal response analysis

To supplement the discussion in the main text, in this appendix we quantify the response of temperature to changes in the parameters of the vertically continuous window-grey atmosphere model in terms of partial derivatives. We thereby also separate the simultaneously occurring effects of CO_2-induced MA cooling in a formal way. We start without the indirect solar effect but include it into the formalism later.

In the following a *response* is simply the partial derivative of temperature with respect to either α_o or β_w. Different responses are discerned based on the conditions introduced into the derivatives. We distinguish between a fast (quasi-instantaneous) response $\mathcal{F}$ where the surface temperature is kept fixed at its previous equilibrium value, and a subsequent slow response $\mathcal{S}$ during which also the surface attains its new equilibrium temperature. The overall equilibrium response $\mathcal{E}$ can thus be written as

$$\mathcal{E} = \mathcal{F} + \mathcal{S}\,. \tag{C1}$$

During the slow transition from $\mathcal{F}$ to $\mathcal{E}$, the current response $\mathcal{C}(t)$ at time t deviates from $\mathcal{E}$ by the transient response $\mathcal{T}(t)$:

$$\mathcal{C}(t) = \mathcal{E} + \mathcal{T}(t)\,, \tag{C2}$$

with

$$\mathcal{T}(t) = \big(f(t) - 1\big)\,\mathcal{S}\,, \tag{C3}$$

where $f(t) \in [0,1]$ is that fraction of the slow response that has already taken effect at time t, with $f(0) = 0$ and $f(t \to \infty) = 1$. The transient response is thus defined as the part of the quasi-instantaneous response that is later compensated by the adjustment to surface warming.

C1 Surface response

Differentiating Eq. (30) with respect to α_o and β_w gives the overall equilibrium responses $\mathcal{E}_{\alpha_o}$ and $\mathcal{E}_{\beta_w}$ at the surface:

$$\mathcal{E}_{\alpha_o,srf} \equiv \frac{\partial T_{srf,eq}}{\partial \alpha_o} = \frac{T_{eff}}{4}\sqrt[4]{\frac{\alpha_o+2}{\alpha_o\beta_w+2}}\left(\frac{1}{\alpha_o+2} - \frac{\beta_w}{\alpha_o\beta_w+2}\right) \tag{C4}$$

and

$$\mathcal{E}_{\beta_w,srf} \equiv \frac{\partial T_{srf,eq}}{\partial \beta_w} = \frac{-T_{eff}\,\alpha_o}{4}\sqrt[4]{\frac{\alpha_o+2}{(\alpha_o\beta_w+2)^5}}\,. \tag{C5}$$

Excluding the trivial cases $\alpha_o = 0$ and $\beta_w = 1$, Eqs. (C4) and (C5) imply that $\mathcal{E}_{\alpha_o,srf} > 0$ and $\mathcal{E}_{\beta_w,srf} < 0$. That is, the surface warms when greenhouse gases are added.

As there is by definition no fast response at the surface, i.e., $\mathcal{F}_{\alpha_o,srf}, \mathcal{F}_{\beta_w,srf} = 0$, it is $\mathcal{S}_{\alpha_o,srf} = (f(t)-1)\mathcal{E}_{\alpha_o,srf}$ and $\mathcal{S}_{\beta_w,srf} = (f(t)-1)\mathcal{E}_{\beta$ the transient response fully compensates for the equilibrium response initially (where $f = 0$), but vanishes for $t \to \infty$.

C2 Atmospheric response

The temperature response of the continuous window-grey atmosphere in overall equilibrium to α_o and β_w as a function of height is obtained by differentiating Eq. (31) with respect to the two model parameters, giving

$$\mathcal{E}_{\alpha_o}(h) \equiv \frac{\partial T_{eq}(h)}{\partial \alpha_o} = \frac{T_{eff,eq}}{4} \sqrt[4]{\frac{\alpha_o(1-h)+1}{\alpha_o\beta_w+2}} \cdot \left(\frac{1-h}{\alpha_o(1-h)+1} - \frac{\beta_w}{\alpha_o\beta_w+2} \right) \tag{C6}$$

and

$$\mathcal{E}_{\beta_w}(h) \equiv \frac{\partial T_{eq}(h)}{\partial \beta_w} = \frac{-T_{eff,eq}\,\alpha_o}{4} \sqrt[4]{\frac{\alpha_o(1-h)+1}{(\alpha_o\beta_w+2)^5}}. \tag{C7}$$

Differentiating the quasi-instantaneous temperature profile given by Eq. (27) in overall equilibrium at $h = 1$ (i.e., at the TOA) with respect to α_o leads to a form that supports the interpretation of the permanent blocking effect as the interplay between the sensitivity of the surface temperature to greenhouse-gases on the one hand and the blocking of upwelling LW radiation by greenhouse gases on the other hand:

$$\mathcal{E}_{\alpha_o,toa} = \sqrt[4]{\frac{1}{\alpha_o+2}} \left(\frac{\partial T_{srf,eq}}{\partial \alpha_o} - \frac{T_{srf,eq}}{4(\alpha_o+2)} \right). \tag{C8}$$

Here the surface sensitivity is represented by the minuend in the brackets whereas the blocking effect is represented by the subtrahend in the brackets.

Differentiating Eq. (27) with respect to α_o under the constraint $T_{srf} = \text{const}$ and inserting Eq. (30) gives the fast temperature response as a function of height:

$$\mathcal{F}_{\alpha_o}(h) \equiv \left. \frac{\partial T(h)}{\partial \alpha_o} \right|_{T_{srf}=T_{srf,eq}=\text{const}} = \frac{T_{eff,eq}}{4} \sqrt[4]{\frac{\alpha_o(1-h)+1}{\alpha_o\beta_w+2}} \left(\frac{1}{\alpha_o+(1-h)^{-1}} - \frac{1}{\alpha_o+2} \right). \tag{C9}$$

Note that changing the width of the atmospheric window entails no fast response, i.e., $\mathcal{F}_{\beta_w}(h) = 0$.

The transient part of the response follows from Eqs. (C6) and (C9) with Eqs. (C1)–(C3) as

$$\begin{aligned}\mathcal{T}_{\alpha_o}(h,t) &\equiv \big(1-f(t)\big)\,\big(\mathcal{F}_{\alpha_o}(h)-\mathcal{E}_{\alpha_o}(h)\big)\\ &= \big(1-f(t)\big)\,\frac{T_{\mathit{eff,eq}}}{4}\sqrt[4]{\frac{\alpha_o(1-h)+1}{\alpha_o\beta_w+2}}\\ &\qquad\cdot\left(\frac{\beta_w}{\alpha_o\beta_w+2}-\frac{1}{\alpha_o+2}\right).\end{aligned} \tag{C10}$$

The transient part of the response therefore becomes smaller with height. Comparison with Eq. (C4) further shows that $|\mathcal{T}_{\alpha_o}(h,t)| < |\mathcal{E}_{\alpha_o,\mathit{srf}}|$, that is, the transient cooling at any height in the atmosphere is always weaker than the equilibrium warming of the surface. Note that $\mathcal{T}_{\beta_w}(h,t)$ follows directly from $\mathcal{E}_{\beta_w}(h)$ because $\mathcal{F}_{\beta_w}(h)=0$.

C3 Inclusion of the indirect solar effect

Considering overall equilibrium, and simplifying the annotation by leaving away h', differentiation of Eq. (38) with respect to the two model parameters gives

$$\mathcal{E}^*_{\alpha_o} \equiv \frac{\partial T^*_{eq}}{\partial \alpha_o} = \left(\frac{T_{eq}}{T^*_{eq}}\right)^3 \mathcal{E}_{\alpha_o} - \frac{s^*}{4{T^*_{eq}}^3\alpha_o^2(1-\beta_w)} \tag{C11}$$

and

$$\mathcal{E}^*_{\beta_w} \equiv \frac{\partial T^*_{eq}}{\partial \beta_o} = \left(\frac{T_{eq}}{T^*_{eq}}\right)^3 \mathcal{E}_{\beta_o} + \frac{s^*}{4{T^*_{eq}}^3\alpha_o(1-\beta_w)^2}, \tag{C12}$$

where $\mathcal{E}_{\alpha_o}$ and $\mathcal{E}_{\beta_w}$ are the window-grey overall equilibrium responses given by Eqs. (C6) and (C7).

To include the indirect solar effect $\mathcal{I}$ into the formalism of Eqs. (C1)–(C3), one can extend Eq. (C2) using Eqs. (38), (C11), and (C12) as follows:

$$\mathcal{C}^*(t) = \underbrace{\mathcal{E}+\mathcal{X}_{\mathcal{EI}}+\mathcal{I}}_{\mathcal{E}^*} + \underbrace{\mathcal{T}(t)+\mathcal{X}_{\mathcal{TI}}(t)}_{\mathcal{T}^*(t)} \tag{C13}$$

with

$$\mathcal{I}_{\alpha_o} = -\frac{s^*}{4{T^*_{eq}}^3\alpha_o^2(1-\beta_w)}, \tag{C14}$$

$$\mathcal{I}_{\beta_w} = \frac{s^*}{4{T^*_{eq}}^3\alpha_o(1-\beta_w)^2}, \tag{C15}$$

$$\mathcal{X}_{\mathcal{EI}} = \left[\left(\frac{T_{eq}}{T^*_{eq}}\right)^3 - 1\right]\mathcal{E}, \tag{C16}$$

$$\mathcal{X}_{\mathcal{TI}}(t) = \left[\left(\frac{T_{eq}}{T^*_{eq}}\right)^3 - 1\right]\mathcal{T}(t), \tag{C17}$$

where the terms in Eqs. (C14)–(C16) follow naturally from Eqs. (C11) and (C12). Equation (C17) results from Eq. (C13) with the analogues of Eqs. (C11) and (C12) for the fast response (i.e., with $\mathcal{E}^*$ and $\mathcal{E}$ replaced by $\mathcal{F}^*$ and $\mathcal{F}$) and the definition of $\mathcal{T}^*(t)$:

$$\mathcal{T}^*(t) = (1 - f(t))(\mathcal{F}^* - \mathcal{E}^*)\,. \tag{C18}$$

The terms $\mathcal{X}_{\mathcal{E}\mathcal{I}}$ and $\mathcal{X}_{\mathcal{T}\mathcal{I}}$ are interaction (or synergy) terms that result from the fact that $\mathcal{E}$, $\mathcal{I}$, and $\mathcal{T}(t)$ are not linearly additive. Due to these terms, the quantitative attribution of a total response to the different mechanisms is not unambiguously possible.

Appendix D: Supporting information on Figure 1

The absorption spectra have been computed with *HITRAN on the Web* (http://hitran.iao.ru). The atmosphere from surface to space (Fig. 1b) was approximated with a 8,000 m thick homogeneous gas mixture at 260 K and 1,013.25 hPa with the following composition (with respect to volume): 4,000 ppm H_2O, 300 ppm CO_2, 0.4 ppm O_3, 0.3 ppm N_2O, 1.7 ppm CH_4, 209,000 ppm O_2, and the remainder N_2. The middle atmosphere (Fig. 1c) was approximated with a 8,000 m thick homogeneous gas mixture at 220 K and 202.65 hPa with the same composition except for H_2O (4 ppm) and O_3 (2 ppm) (and correspondingly N_2). Some Gaussian smoothing was applied to the spectra.

Acknowledgements. The foundations for this work have been laid during the authors' employment at the Max Planck Institute for Meteorology, Hamburg, Germany. The ECHAM6 simulations have been conducted at the German Climate Computing Centre (DKRZ). We thank Stephan Bakan and Thomas Rackow for helpful discussions, and Sebastian Rast for technical support with ECHAM6. Thanks are also extended to Angus Ferraro, Max Popp, and an anonymous reviewer for very constructive comments.

References

Beig, G.: Long-term trends in the temperature of the mesosphere/lower thermosphere region: 1. Anthropogenic influences, Journal of Geophysical Research: Space Physics, 116, 2011.

Beig, G., Keckhut, P., Lowe, R. P., Roble, R. G., Mlynczak, M. G., Scheer, J., Fomichev, V. I., Offermann, D., French, W. J. R., Shepherd, M. G., Semenov, A. I., Remsberg, E. E., She, C. Y., Lübken, F. J., Bremer, J., Clemesha, B. R., Stegman, J., Sigernes, F., and Fadnavis, S.: Review of mesospheric temperature trends, Rev. Geophys., 41, 2003.

Dickinson, R. E., Liu, S. C., and Donahue, T. M.: Effect of Chlorofluoromethane Infrared Radiation on Zonal Atmospheric Temperatures, J. Atmos. Sci., 35, 2142–2152, doi:10.1175/1520-0469(1978)035<2142:EOCIRO>2.0.CO;2, 1978.

Fels, S. B., Mahlman, J. D., Schwarzkopf, M. D., and Sinclair, R. W.: Stratospheric Sensitivity to Perturbations in Ozone and Carbon Dioxide: Radiative and Dynamical Response, J. Atmos. Sci., 37, 2265–2297, doi:10.1175/1520-0469(1980)037<2265:SSTPIO>2.0.CO;2, 1980.

Ferraro, A. J., Collins, M., and Lambert, F. H.: A hiatus in the stratosphere?, Nature Climate Change, 5, 497–498, 2015.

Forster, F., Piers, M., and Shine, K. P.: Radiative forcing and temperature trends from stratospheric ozone changes, Journal of Geophysical Research: Atmospheres, 102, 10 841–10 855, 1997a.

Forster, P. M. and Joshi, M.: The role of halocarbons in the climate change of the troposphere and stratosphere, Climatic Change, 71, 249–266, doi:10.1007/s10584-005-5955-7, 2005.

Forster, P. M., Bodeker, G., Schofield, R., Solomon, S., and Thompson, D.: Effects of ozone cooling in the tropical lower stratosphere and upper troposphere, Geophys. Res. Lett., 34, L23 813, doi:10.1029/2007GL031994, 2007.

Forster, P. M. F., Freckleton, R. S., and Shine, K. P.: On aspects of the concept of radiative forcing, Clim. Dyn., 13, 547–560, doi:10.1007/s003820050182, 1997b.

Gillett, N. P., Allen, M. R., and Williams, K. D.: Modelling the atmospheric response to doubled CO_2 and depleted stratospheric ozone using a stratosphere-resolving coupled GCM, Q.J.R. Meteorol. Soc., 129, 947–966, doi:10.1256/qj.02.102, 2003.

Goody, R. M. and Yung, Y. L.: Atmospheric Radiation, Oxford University Press, 1989.

Hansen, J., Sato, M., and Ruedy, R.: Radiative forcing and climate response, Journal of Geophysical Research: Atmospheres, 102, 6831–6864, 1997.

Huang, F. T., Mayr, H. G., Russell III, J. M., and Mlynczak, M. G.: Ozone and temperature decadal trends in the stratosphere, mesosphere and lower thermosphere, based on measurements from SABER on TIMED, Ann. Geophys, 32, 935–949, doi:10.5194/angeo-32-935-2014, 2014.

Iacono, M. J., Delamere, J. S., Mlawer, E. J., Shephard, M. W., Clough, S. A., and Collins, W. D.: Radiative forcing by long-lived greenhouse gases: Calculations with the AER radiative transfer models, J. Geophys. Res. Atm., 113, 2008.

Liou, K. N.: An Introduction to Atmospheric Radiation, vol. 84, Academic Press, 2002.

Liu, Q. and Weng, F.: Recent Stratospheric Temperature Observed from Satellite Measurements, SOLA, 5, 53–56, doi:10.2151/sola.2009, 2009.

Manabe, S. and Strickler, R. F.: Thermal Equilibrium of the Atmosphere with a Convective Adjustment, J. Atmos. Sci., 21, 361–385, doi:10.1175/1520-0469(1964)021<0361:TEOTAW>2.0.CO;2, 1964.

Manabe, S. and Wetherald, R. T.: Thermal Equilibrium of the Atmosphere with a Given Distribution of Relative Humidity, J. Atmos. Sci., 24, 241–259, doi:10.1175/1520-0469(1967)024<0241:TEOTAW>2.0.CO;2, 1967.

Manabe, S. and Wetherald, R. T.: The effects of doubling the CO_2 concentration on the climate of a general circulation model, J. Atmos. Sci., 32, 3–15, doi:10.1175/1520-0469(1975)032<0003:TEODTC>2.0.CO;2, 1975.

Maycock, A. C., Shine, K. P., and Joshi, M. M.: The temperature response to stratospheric water vapour changes, Q.J.R. Meteorol. Soc., 137, 1070–1082, doi:10.1002/qj.822, 2011.

Mlynczak, M. G.: A contemporary assessment of the mesospheric energy budget, Geoph. Monog. Series, 123, 37–52, doi:10.1029/GM123p0037, 2000.

Neelin, J. D.: Climate Change and Climate Modeling, Cambridge University Press, 2011.

Pierrehumbert, R. T.: Principles of Planetary Climate, Cambridge University Press, 2010.

Pollack, J. B.: Temperature structure of nongray planetary atmospheres, Icarus, 10, 301–313, doi:10.1016/0019-1035(69)90031-1, 1969a.

Pollack, J. B.: A nongray CO_2-H_2O greenhouse model of Venus, Icarus, 10, 314–341, doi:10.1016/0019-1035(69)90032-3, 1969b.

Pujol, T. and North, G. R.: Runaway greenhouse effect in a semigray radiative-convective model, J. Atmos. Sci., 59, 2801–2810, doi:10.1256/qj.02.144, 2002.

Ramaswamy, V. and Schwarzkopf, M. D.: Effects of ozone and well-mixed gases on annual-mean stratospheric temperature trends, Geophys. Res. Lett., 29, 2064, doi:10.1029/2002GL015141, 2002.

Ramaswamy, V., Schwarzkopf, M., and Shine, K.: Radiative forcing of climate from halocarbon-induced global stratospheric ozone loss, Nature, 1992.

Ramaswamy, V., Chanin, M.-L., Angell, J., Barnett, J., Gaffen, D., Gelman, M., Keckhut, P., Koshelkov, Y., Labitzke, K., Lin, J.-J. R., O'Neill, A., Nash, J., Randel, W., Rood, R., Shine, K., Shiotani, M., and Swinbank, R.: Stratospheric temperature trends: observations and model simulations, Rev. Geophys., 39, 71–122, doi:10.1029/1999RG000065, 2001.

Randel, W. J., Shine, K. P., Austin, J., Barnett, J., Claud, C., Gillett, N. P., Keckhut, P., Langematz, U., Lin, R., Long, C., Mears, C., Miller, A., Nash, J., Seidel, D. J., Thompson, D. W. J., Wu, F., and Yoden, S.: An update of observed stratospheric temperature trends, J. Geophys. Res., 114, D02 107, doi:10.1029/2008JD010421, 2009.

Sagan, C.: Gray and nongray planetary atmospheres structure, convective instability, and greenhouse effect, Icarus, 10, 290–300, 1969.

Salby, M. L.: Radiative transfer, In: Climate System Modeling, K. E. Trenberth, Ed., chap. 3.4, pp. 88–94, Cambridge University Press, 1992.

Santer, B. D., Painter, J. F., Mears, C. A., Doutriaux, C., Caldwell, P., Arblaster, J. M., Cameron-Smith, P. J., Gillett, N. P., Gleckler, P. J., Lanzante, J., Perlwitz, J., Solomon, S., Stott, P. A., Taylor, K. E., Terray, L., Thorne, P. W., Wehner, M. F., Wentz, F. J., Wigley, T. M. L., Wilcox, L. J., and Zou, C.-Z.: Identifying human influences on atmospheric temperature, Proceedings of the National Academy of Sciences, doi:10.1073/pnas.1210514109, 2012.

Seidel, D. J., Gillett, N. P., Lanzante, J. R., Shine, K. P., and Thorne, P. W.: Stratospheric temperature trends: our evolving understanding, WIREs Clim Change, 2, 592–616, doi:10.1002/wcc.125, 2011.

Shine, K. P., Bourqui, M. S., Forster, P. M. d. F., Hare, S. H. E., Langematz, U., Braesicke, P., Grewe, V., Ponater, M., Schnadt, C., Smith, C. A., Haigh, J. D., Austin, J., Butchart, N., Shindell, D. T., Randel, W. J., Nagashima, T., Portmann, R. W., Solomon, S., Seidel, D. J., Lanzante, J., Klein, S., Ramaswamy, V., and Schwarzkopf, M. D.: A comparison of model-simulated trends in stratospheric temperatures, Q.J.R. Meteorol. Soc., 129, 1565–1588, doi:10.1256/qj.02.186, 2003.

Stevens, B., Giorgetta, M., Esch, M., Mauritsen, T., Crueger, T., Rast, S., Salzmann, M., Schmidt, H., Bader, J., Block, K., Brokopf, R., Fast, I., Kinne, S., Kornblueh, L., Lohmann, U., Pincus, R., Reichler, T., and Roeckner, E.: Atmospheric component of the MPI-M Earth System Model: ECHAM6, Journal of Advances in Modeling Earth Systems, 5, 146–172, doi:10.1002/jame.20015, http://dx.doi.org/10.1002/jame.20015, 2013.

Stolarski, R. S., Douglass, A. R., Newman, P. A., Pawson, S., and Schoeberl, M. R.: Relative contribution of greenhouse gases and ozone-depleting substances to temperature trends in the stratosphere: a chemistry-climate model study, J. Climate, 23, 28–42, doi:10.1175/2009JCLI2955.1, 2010.

Stuber, N., Sausen, R., and Ponater, M.: Stratosphere adjusted radiative forcing calculations in a comprehensive climate model, Theoretical and applied climatology, 68, 125–135, 2001.

Thomas, G. E. and Stamnes, K.: Radiative Transfer in the Atmosphere and Ocean, Cambridge University Press, 1999.

Thompson, D. W. J. and Solomon, S.: Recent Stratospheric Climate Trends as Evidenced in Radiosonde Data: Global Structure and Tropospheric Linkages, J. Climate, 18, 4785–4795, doi:10.1175/JCLI3585.1, 2005.

Thompson, D. W. J. and Solomon, S.: Understanding Recent Stratospheric Climate Change, J. Climate, 22, 1934–1943, doi:10.1175/2008JCLI2482.1, 2009.

Thompson, D. W. J., Seidel, D. J., Randel, W. J., Zou, C.-Z., Butler, A. H., Mears, C., Osso, A., Long, C., and Lin, R.: The mystery of recent stratospheric temperature trends, Nature, 491, 692–697, doi:10.1038/nature11579, 2012.